

CHARACTERISTICS OF A HIGH-ENTHALPY ELECTRIC-ARC HEATER FOR AIR AT ATMOSPHERIC PRESSURE

V. L. Sergeev

UDC 533.951.7:536.24.01

A vortex-type plasma generator is described, and its current-voltage and heat characteristics as well as the basic parameters of the plasma jet are reported. Results of an investigation of the heater are compared with literature data. Correlations for the basic characteristics are derived that may be employed to design a high-enthalpy plasma generator.

In the reentry of space vehicles into dense layers of the atmosphere the increase in the parameters of the plasma jet (in particular, the enthalpy) is determined by the enthalpy and stagnation pressure of air near the stagnation point. At the pressure 10^5 N/m^2 the enthalpy in the stagnation-point region attains 26,000 kJ/kg for a satellite, 32,000 kJ/kg for an intercontinental ballistic missile, and 90,000 kJ/kg for an interplanetary probe [1, 2]. The stagnation pressure changes from less than 10^5 N/m^2 to $(50-60) \cdot 10^5 \text{ N/m}^2$. The increase in the enthalpy is also an urgent problem in some other applications of a plasma generator. The temperature of air heated in a linear-circuit plasma generator is approximately 6000 K at atmospheric pressure [3], which corresponds to an enthalpy of 15,000 kJ/kg.

As is reported for some linear-circuit plasma generators (including those with interelectrode insertions (IEI) [4-12], the enthalpy of heated air is 3500 to 25,000 kJ/kg. In the survey [13] plasma generators are mentioned in which air and nitrogen are heated to $(30-40) \cdot 10^3 \text{ kJ/kg}$ at atmospheric pressure.

A comparison of the parameter values required for the studies of heat-shielding materials and the values attained using the above installations demonstrates the necessity of further investigations on an increase in the enthalpy of air heated in plasma generators. From the viewpoint of the attained enthalpies of heated air, plasma generators with IEIs and porous cooling of the channel show no substantial advantages over other designs of a linear-circuit plasma generator.

A simple increase in the applied power does not resolve the problem of increasing the enthalpy, as evidenced by the parameters of powerful installations. The increase in the power, with the channel geometry unchanged, is limited by the maximum permissible heat fluxes toward the channel wall. The same reason restricts the possibilities of increasing the enthalpy by decreasing the diameter of the channel and of the interelectrode insertion. The pressure in the discharge chamber imposes substantial constraints on the maximum enthalpy of the gas. Whereas at a chamber pressure close to atmospheric the limiting mean enthalpy of the heated gas is estimated as approximately 35,000 kJ/kg, at a pressure of $100 \cdot 10^5 \text{ N/m}^2$ it decreases to 5000 kJ/kg [14]. Below we consider a method of increasing the enthalpy of the heated gas with the aid of a jet core.

In the investigation we employed a linear-circuit vortex-type electric-arc gas heater, one of whose variants with welded electrodes is shown schematically in Fig. 1. The electrodes were of identical design and were segments of thick-walled copper tubes water-cooled on the outside. The electrode length varied from 50 to 230 mm, and the channel diameter varied from 10 to 30 mm. The cathode was graphite-plugged. The 20-mm-long plug did not practically burn out. Swirled gas (nitrogen, air) was supplied to a 1-7-mm gap between the electrodes at $G = 1.8-14 \text{ g/sec}$.

Academic Scientific Complex "A. V. Luikov Heat and Mass Transfer Institute, Academy of Sciences of Belarus," Minsk. Translated from *Inzhenerno-Fizicheskii Zhurnal*, Vol. 66, No. 5, pp. 590-599, May, 1994. Original article submitted January 15, 1993.

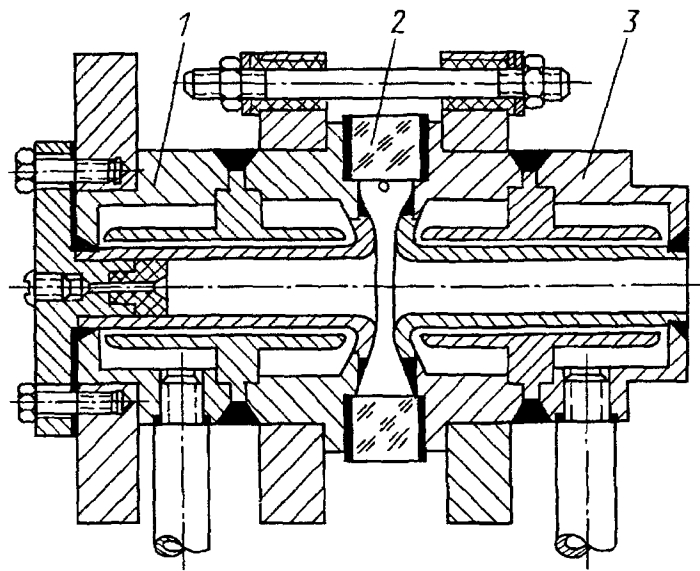


Fig. 1. Schematic of a linear-circuit vortex-type plasma generator: 1) cathode; 2) gas ring; 3) anode.

The gas rings were made of textolite, organic glass, fiber glass, and metal. The internal diameter of a gas ring varied from 44 to 86 mm. The gas was fed tangentially to the inner surface via holes in the gas ring. The number of 4-mm-diameter holes varied from one to four. To investigate the effect of the IEIs on the jet parameters, we used interelectrode insertions with a channel diameter of 10, 15, 20 mm and a length of 22 mm. Swirled gas was injected into the gaps between the IEIs. The number of insertions varied from 0 to 5. The position of the reference arc spot in the channel was investigated with the aid of sectioned electrodes. With an anode length of 230 mm the number of sections amounted to 11. Power was supplied to the discharge chambers from mercury rectifiers with the parameters: $I_{\text{rated}} = 1500$ A, $U_{\text{rec}} = 480$ and 825 V, $N = 40\text{--}300$ kW.

For each section of the IEIs and the electrodes we measured the flow rate and heating temperature of the cooling water. Using a light-beam oscillograph, we also recorded the current, voltage, and potentials of the IEI sections relative to the electrodes. The position of the arc was determined by the current and heat flux distribution along the channel.

The mean enthalpy at the outlet was calculated from the heat balance of the plasma generator. The enthalpy (temperature) in the jet core was measured by two noncontact methods (by the method of relative intensity of spectral lines and from broadening of the H_{β} line) and two contact methods (by Grey's method and from the heat flux and pressure near the stagnation point with the use of Fay and Riddle's dependence). The heat flux near the stagnation point was determined by the exponential method. To determine the enthalpy distribution over the radius and length of the plasma jet, we used a multifunctional pickup that allowed simultaneous measurement of three variable parameters: heat flux, stagnation pressure, and flux enthalpy [15]. The pickup recorded changes in the pressure of tenth to hundredths of an atmosphere at frequencies up to 400 Hz and in heat flux up to 150 Hz. Signals were recorded in time by an oscillograph, model HO30A. The jet velocity was determined from the dynamic head and the gas density calculated from the enthalpy.

The error in determining the stagnation pressure amounted to 2%, the heat flux 10%, the gas enthalpy 12–15% depending on the method, and the jet velocity 7%.

The methods of measuring the jet parameters are considered in detail in [15].

Current-voltage characteristics obtained at a current strength of 150 to 1300 A and a gas flow rate of 2 to 10 g/sec (the geometric parameters are given above) are described by the relation

$$\frac{Ud}{I} = A \left(\frac{I^2}{Gd} \right)^n, \quad (1)$$

where $A = 955$, $n = -0.655$. The maximum deviation of the voltage calculated by the formula from the experimental curves does not exceed 10%.

Many correlations have been proposed (see [16–22] and others) for calculating new linear-circuit plasma generators operating with air. In all, 16 dependences have been used (see [23], Table 1). These data were used to calculate the current-voltage characteristics of the plasma generator investigated and for comparison with formula (1). From some works it follows that the influence of the anode diameter is insignificant, and it has not been included in processing the characteristics (or it may be eliminated in the final formula). For the basic group of dependences the deviation from the experimental curve is 15–35%. The difference in the calculation results (for the linear-circuit plasma generator and chamber pressures from 10 to 0.42 N/cm²) attains 60%. It is pertinent to note that we deal with one concrete design of a plasma generator but in the literature one may come across formulas recommended for calculating, with a rather high accuracy, characteristics for dissimilar plasma generators and various gases. The relation obtained from processing the generalized characteristics of various authors is close to formula (1) ($A = 935$, $n = 0.7$). When the formula included, in addition to the two basic combinations, other multipliers, we calculated two characteristics for the two extreme values of the parameters or for the mean value of the correction. The dependence presented may be used to calculate current-voltage characteristics for an air flow rate ranging from 2 to 10 g/sec, electrode diameters from 10 to 30 mm, a discharge chamber pressure from 10 to 15 N/cm², an electrode gap from 1 to 3 mm, and a current strength from 100 to 1500 A.

As a result of measuring the distributions of the current strength and heat losses along the sectioned electrodes, we have obtained a correlation for arc length ($d = 15–20$ mm):

$$l_g = -0.435I + 24G + 230, \quad (2)$$

which generalizes experimental data with an error of 10–20%. As measurements have shown, the electric intensity distribution along the arc is *U*-shaped. With a decrease in the current strength, the region with a constant electric intensity enlarges. The areas with an increase are associated with a near-electrode drop in the voltage. As a function of the gas flow rate and the current strength, the mean electric intensity varies within 10 to 30 V/cm [23].

Data on the heat flux distribution along the electrodes allow evaluation of heat losses in the reference arc spot and the effective near-electrode drop in the voltage. The losses in the reference spot of the anode make up 20–30% of the total losses and are practically independent of the current strength in the range 200–800 A. Based on experimental data, the effective near-electrode voltage drop, including the near-electrode drop proper, the work function, the thermal energy of the electrons, and the voltage drop over the part of the arc transverse to the flux, is

$$\Delta U_{an}^{ef} = 0.0171I + 17.3. \quad (3)$$

The data obtained allow evaluation of the minimum anode length [23] as a function of the specified mean enthalpy of the heated gas, the power, and the gas flow rate.

The current-voltage characteristics are limited by the blowing-out of the arc from the channel with a decrease in the current strength and by an increase in the gas flow rate and entry of the arc into the interelectrode gap upon a reverse change in the indicated parameters. An increase in the gas ring diameter entails a change in the range of operating conditions. With an interelectrode gap $\delta \leq 1$ mm, the range of operating parameters is narrower since gap breakdown may easily occur. With an increase of the gap to a certain value, the range of operating parameters broadens. With an anode diameter of 30 mm and a length of 100 mm the arc is easily blown out of the channel.

Each of the enumerated parameters has an optimum value in the investigated gas flow rate and current ranges. The optimum values for the anode and cathode diameters are 15–20 mm, for interelectrode gap 1.5–2.5 mm, and for the gas ring diameter 74 mm. In [24], domains of operating conditions are given as a function of the gas flow rate and geometric parameters.

Processing of the experimental data on heat losses to electrodes showed that they fall on a single straight line as a function of the current for different gas flow rates but branch off as a function of the channel diameter. As a result, the dependence for the specific heat flux to the anode is

$$q_{an} = 0.4I^{1.2}/10^{3.9d}, \quad (4)$$

and for heat losses in the discharge chamber we have

$$\frac{Q_{d.ch}}{L} = 0.93 \left(\frac{I}{100} \right)^{\frac{d}{20}+1.05} \cdot 10^{-0.17d}. \quad (5)$$

The ratio of heat losses in the anode to those in the discharge chamber for anode of diameters 10–30 mm is directly proportional to the current strength:

$$Q_{an}/Q_{d.ch} = 8 \cdot 10^{-5}I + 0.45 \quad (6)$$

or is approximately equal to 0.5 in the investigated range of current strengths. An increase in the gas flow rate at a constant power leads to a decrease in the enthalpy and an increase in the gas velocity. As a result, with an increase in the flow rate at a constant power the losses decrease. Moreover, with a decrease in the current strength the losses at the reference point of the arc decrease. As processing of the experimental data on the mean enthalpy of the heated gas has revealed, the power dependences of the enthalpy have maxima, which may be explained by an advanced increase in the losses with an increase of the power. The maximum enthalpy values are within the limits 17,000–21,000 kJ/kg for the investigated N/G range 30–55 kW·sec/g and are determined by this ratio independently of the electrode diameter. The power corresponding to the maximum enthalpy is related to the gas flow rate for $d_{an} = 10–30$ mm by

$$N_{H_{max}} = 31.6G + 33.8. \quad (7)$$

Processing of the data on heat losses to the heater anode with vortex stabilization of the discharge has yielded in dimensionless form the relation

$$St = (6.87 - 0.611 \cdot 10^{-3} Re) \left(3.4 \frac{d}{l} + 0.32 \right) \cdot 10^{-3} \exp(0.923 \cdot 10^{-2} N/GH_0), \quad (8)$$

where

$$St = \frac{Q_{an}}{IU - Q_c} \frac{d}{4l}; \quad Re = \frac{4G}{\pi d \bar{\mu}}; \quad (9)$$

$$l/d = 3.5–10; \quad Re = 500–8000; \quad N/GH_0 = 40–165.$$

The dependence of the heat losses in the spot on the current strength for flow rates of 2–7 g/sec and anode diameters of 10–20 mm is described by the relation

$$Q_s = 1.25 \cdot 10^{-3} I^{1.51}. \quad (10)$$

In our case, heat losses in the reference spot are approximately equal to convective losses, i.e., displacement of the reference spot over the electrode surface with the aid of a gas vortex is rather effective and allows the mean specific flux in the reference spot to be reduced to the permissible level.

In [12] it is shown that the efficiency of a vortex-type plasma generator is determined by the following dimensionless combinations:

$$\eta = 1 - \frac{Q_{an}}{N} - \frac{Q_c}{N} = f \left(\frac{I^2}{Gh_0\sigma_0 d}, \text{Re}, \text{Pr}, \frac{h_w}{h}, m, n, \text{etc.} \right). \quad (11)$$

For the kind of gas under consideration, the heat losses to the electrode [23] may be written, proceeding from (11), as

$$\frac{Q_{el}}{N} = \varphi \left(\frac{I^2}{Gdh_0\sigma_0}, \frac{G}{d\mu_0}, \frac{l}{d} \right). \quad (12)$$

The parameters h_0 , σ_0 , and μ_0 are assumed to have some constant values. The range of operating and geometric parameters given above corresponded to the following ranges of the quantities in expression (12): $I^2/Gd = 400-45,000 \text{ A}^2 \cdot \text{sec}/\text{g} \cdot \text{mm}$, $G/d = 0.09-1.0 \text{ g}/\text{sec} \cdot \text{mm}$, $l/d = 3.3-20$, $Q_{an}/N = 0.12-0.43$, $Q_c/N = 0.2-0.3$.

From the data obtained it follows that the heat losses to the anode decrease with an increase in G/d and increase somewhat with an increase in l/d and I^2/Gd . The characteristic value of the enthalpy h_0 may be found by comparing the determination of Re by (9) with the experimental relation obtained for it

$$\text{Re} = 7.47 \cdot 10^3 G/d. \quad (13)$$

Hence $\mu_0 = 17.1 \cdot 10^{-5} \text{ kg}/(\text{m} \cdot \text{sec})$ and $T_0 = 6640 \text{ K}$.

The experimental data for the anode are described, with an error of up to 18%, by the expression

$$\frac{Q_{an}}{N} = 0.05 \left(\frac{I^2}{Gd} \right)^{0.11} \left(\frac{G}{d} \right)^{-0.25} \left(\frac{l}{d} \right)^{0.17}, \quad (14)$$

and for the cathode by

$$\frac{Q_c}{N} = 0.141 (I^2/Gd)^{0.06}. \quad (15)$$

A comparison of (14) and (15) with the relation for the efficiency of a linear-circuit plasma generator [25] testifies to their satisfactory agreement. The discrepancy in the efficiency does not exceed 17% for I^2/Gd in the range from 1000 to 27,000.

Since such experimental dependences as (11) include many parameters, some of which are unknown a priori in the calculation of a new plasma generator (e.g., h , Pr in (11) and the discharge chamber pressure in some other formulas in the literature), their use involves difficulties. Therefore, expressions for the efficiency that are based on the general gasdynamic relations may be of help.

Under the assumption of subsonic efflux, combining the Bernoulli equation and the formula for the flow rate and using the enthalpy dependence of the density of nitrogen

$$\rho = 14.8h^{-0.605}, \quad T = 3000 - 8000 \text{ K}, \quad (16)$$

we obtain the following expression for enthalpy of the heated gas:

$$h = 115 (p - p_*)^{1.65} d^{6.6} (10^3 G)^{-3.3}, \quad (17)$$

$$\eta = 236 (p - p_*)^{1.65} d^{6.6} (10^3 G)^{-2.3} N^{-1}, \quad (18)$$

where $p \cdot 9.81$ is given in N/cm^2 , G in kg/sec , and p_* is atmospheric pressure.

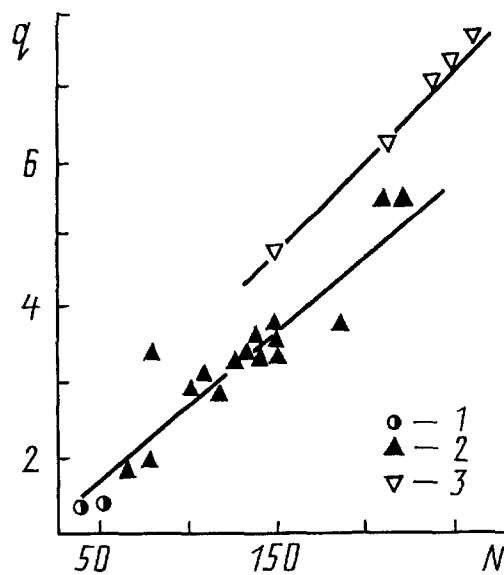


Fig. 2. Heat flux from the plasma jet to the obstacle near the stagnation point, $d_{an} = 15$ mm: 1) $G = 2.5$ g/sec; 2) 5; 3) 7. q , kW/cm²; N , kW.

As a comparison of the results calculated by (17), (18) and the experimental data [23] (Fig. 20) shows, the formulas derived are applicable for calculation of plasma generators. It is noteworthy that these formulas are obtained without using experimental data for concrete designs of plasma generators and are of a general character.

Analogous dependences that are consistent with the experimental data of the present author and other researchers [23] may be obtained for the sonic efflux of air:

$$h = \frac{1}{1260} p^{2.94} d^{5.88} G^{-2.94}, \quad (19)$$

$$\eta = \frac{1}{1260} p^{2.94} d^{5.88} G^{-1.94} N^{-1}. \quad (20)$$

The above expressions for the enthalpy allow determination of its mean values at the outlet of a plasma generator.

For our purposes it is important to know the enthalpy in the jet core and the influence of the basic parameters of the plasma generator on it.

For a plasma generator with welded electrodes (Fig. 1) we determined the enthalpy in the jet core at a distance of 10 mm from the nozzle section by using the heat flux (Figs. 2, 3) toward a 3-mm diameter pickup protected from lateral heating with a spherically rounded ($R = 1$ cm) textolite sleeve, the stagnation pressure measured by a pickup of the same shape and dimensions, and the relation $q = f(h_0, p_0, R)$ from [15]:

$$q = 4.5 \cdot 10^{-4} R^{-0.5} p_0^{0.25} (p_0 - p_\infty)^{0.25} (h_0 - h_w). \quad (21)$$

In addition to determination of the enthalpy using the heat transfer relationship, we also measured it by a Grey pickup (Fig. 3, points 5) and by the method of relative intensity of spectral lines (points 6) [23]. The results obtained show good agreement for the measurements by the contact and noncontact methods.

The experiments demonstrated that the jet core enthalpy increases with an increase in the power and the gas flow rate. It is noteworthy that the effect of the flow rate is more substantial on the formation of a high-enthalpy core of the jet.

As the measurement results show, isolation of the central part of the jet by a colder gas layer by a proper choice of the plasma generator parameters makes it possible to obtain for tens of minutes a jet core whose enthalpy exceeds substantially (by a factor of 3–6, Fig. 3) the mean enthalpy of the heated gas and to use it for

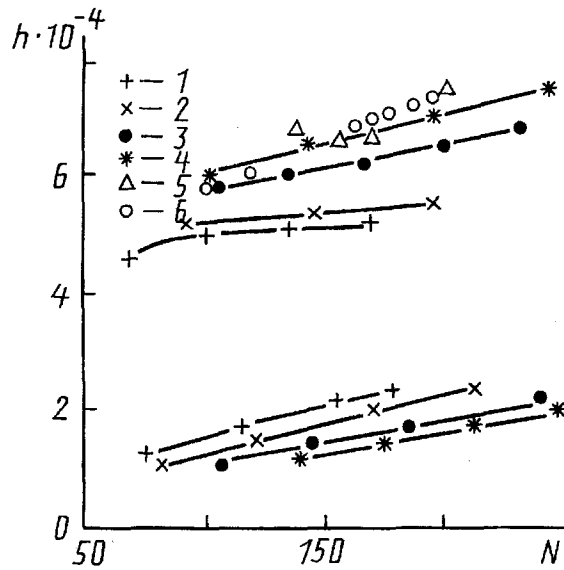


Fig. 3. Enthalpy of the jet versus discharge power and gas flow rate, $d_{an} = 20$ mm: 1) $G = 3.5$ g/sec; 2) 4.5; 3) 6; 4, 5, 6) 7; 1-4) determination from the heat flux and the stagnation pressure; 5) Grey pickup; 6) spectroscopic method. Upper curves pertain to the jet core; lower curves indicate mean enthalpies. h , kJ/kg.

investigations. The considered method of increasing the jet enthalpy may be used together with other methods for increasing the parameters. However unlike those methods, it does not require an increase in the power, the voltage of the power unit, or the heat resistance of the channel wall.

Using the combinations of parameters from the solution for enthalpy distribution in the plasma generator channel [26], we may approximate the relations obtained for the enthalpy in the jet core at the nozzle section by the generalized expression

$$\frac{h_{0m}d}{(IG)^{0.5}} = 3260G^{-0.353} \left(\frac{I^2}{Gd} \right)^{-0.122} \quad (22)$$

An investigation of a plasma generator with interelectrode insertions has shown [24] that the effect of an IEI on the jet characteristics is ambiguous. For a plasma generator with IEIs, the ratio $h_{0m}/\bar{h} = 1.5-3$, which is substantially smaller than for a plasma generator without IEIs with all the other conditions being equal. This is possibly due to the fact that the longer arc and the distributed gas delivery in a plasma generator with IEIs allow more uniform heating of the gas over the cross section. On the other hand, an IEI stabilizes the arc, causes a 1.5-2-fold decrease in the fluctuations of the jet temperature, and creates a rising section of the current-voltage characteristic.

When using plasma jets in tests of heat-shielding materials and in other technological processes one must know, in addition to the enthalpy and the stagnation pressure, the heat flux to the tested piecework. An example of measuring this heat flux is shown in Fig. 2.

The generalized dependence of the heat flux on the plasma generator parameters and the obstacle dimensions for air and nitrogen may be represented as

$$q_0 = 10^3 d^{-0.22} (G/d)^{0.98} (I^2/Gd)^{0.4} R^{-0.5}, \quad (23)$$

where d is expressed in m; G in kg/sec. The heat flux from the jet to the obstacle near the stagnation point increases with the current and the gas flow rate and decreases with an increase in the anode diameter. It is noteworthy that the heat flux depends on the current strength to a greater extent than on the gas flow rate.

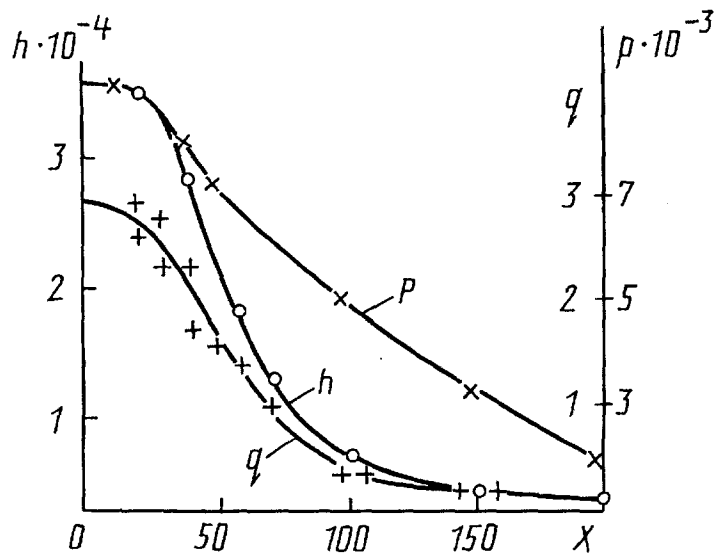


Fig. 4. Illustrating the heat flux, stagnation pressure, and enthalpy distributions along the jet: $d_{an} = 20$ mm, $N = 176$ kW, $G = 10$ g/sec. p , N/m^2 ; x , mm.

The heat flux to the plane end face of a cylinder of radius R (the shape typical of specimens of heat-shielding materials) is related to the heat flux to a sphere of radius R (23) by the expression $q_{pl}/q_{sp} = 0.65$ [15].

In using a plasma jet, it is necessary to know, in addition to the parameters at the nozzle section, their distribution along the axis and over the radius of the jet. The distributions of the heat fluxes, pressure, and enthalpy were measured with the aid of the aforementioned multifunctional pickup, which allowed variable parameters to be measured, by displacing it along the jet diameter or its axis (Fig. 4).

The experiments showed that the enthalpy distributions over the radius are similar to those along the jet and are approximated by Gaussian curves:

$$h/h_m = \exp [- \ln 2 (r/r_{0.5h_m})^2], \quad (24)$$

where the thermal half-width of the jet is

$$r_{0.5h_m}(x) = r_{0.5h_{0m}} + 2.74 \cdot 10^{-6} r_0 \left(\frac{x}{r_0} \right)^{0.95} \left(\frac{h_{0m}}{h_\infty} \right)^{1.56}. \quad (25)$$

The enthalpy distribution along the jet axis (near the axis) is described by the relation

$$h_{xm}/h_{0m} = \exp [- 0.004 (x/r_0)^{2.3}]. \quad (26)$$

The results of the experiments are consistent with the calculated distributions of the parameters in the jet and also with experimental data of other authors [27].

As is seen from the heat flux distribution along the jet axis (Fig. 4), the jet may be divided into three zones: an initial zone, where the heat flux is constant, a transition zone, and a zone of exponential change of the heat flux. The heat flux distribution over the third (main) zone is described by the expression

$$\frac{q}{q_{03}} = 1.9 \exp \left\{ - \left[0.031G + 0.85 (0.15 + 0.2R_p + 0.0026G) \frac{x}{d} \right] \right\}. \quad (27)$$

The resistance of the loading regulator R_p is related to the gas flow rate and the discharge power by the dependence

$$N = \frac{165}{R_p} (1 - 3.32 e^{-0.42G}), \quad (28)$$

found experimentally. Formula (27) describes the experimental data, with an error of $\pm 20\%$, for air with a flow rate from 6 to 16 g/sec, for a discharge power from 100 to 270 kW, and for a nozzle diameter of 15–20 mm.

The boundary of the main jet zone may be estimated by the relation

$$\left(\frac{x}{d}\right)_b \frac{1}{G} = 1.35 - 0.883R_p - 0.05G. \quad (29)$$

Since the initial zone is usually small, relation (29) also allows estimation of the length of the transition zone of the jet.

When the initial and transition zones are absent, the heat flux distribution along the jet axis may also be estimated by the expression

$$q_x/q_0 = \exp[-0.126(x/d)^{1.5}]. \quad (30)$$

The plasma generator developed makes it possible to investigate the destruction characteristics of heat-shielding materials of various compositions in a wide range of enthalpies of the heated gas. For instance, in experiments with 14-mm-diameter samples of materials, the enthalpy of the heated gas attained 50,000 kJ/kg.

NOTATION

I , current strength, A; l_g , arc length, mm; Q_{an} , Q_c , $Q_{d.ch.}$, Q_s , heat losses in the anode, cathode, discharge chamber, and reference spot of the arc, respectively, kW; l , anode length, cm; d , anode diameter, cm; G , gas flow rate, g/sec; N , arc power, kW; $H_0 = 335$ kJ/kg, enthalpy of the cold gas; q , specific heat flux, kW/cm²; L , length of the discharge chamber, cm; $\bar{\mu}$, gas viscosity based on the mean-mass temperature of the heated gas; R , radius of rounding of the nose of the pickup, m; p_0 , stagnation pressure, N/m²; h_0 , stagnation enthalpy, kJ/kg; h_{0m} , axial enthalpy of the gas near the nozzle section; h_{xm} , near-axis enthalpy at the distance x from the nozzle; q_{03} , heat flux in the initial cross section of the third zone of the jet; R_p , resistance of the loading regulator, Ω .

REFERENCES

1. J. A. Fay and N. H. Kemp, *Mekhanika*, No. 1, 47-70 (1964).
2. M. C. Adams, *Vopr. Raket. Tekh.*, No. 2, 25-36 (1962).
3. A. G. Shashkov, O. I. Yas'ko, V. L. Sergeev, and F. B. Yurevich, *Inzh.-Fiz. Zh.*, 5, No. 2, 115-129 (1962).
4. A. L. Mosse, L. D. Kul'batskii, S. A. Fedorov, et al., in: *Investigations of Plasma Processes and Apparatuses* [in Russian], Collected Papers of the Academic Scientific Complex "Heat and Mass Transfer Institute of the Academy of Sciences of Belarus," Minsk (1991), pp. 87-98.
5. A. P. Iskrenkov, N. A. Kostin, and V. V. Toropov, in: *Investigations of Plasma Processes and Apparatuses* [in Russian], Collected Papers of the Academic Scientific Complex "Heat and Mass Transfer Institute of the Academy of Sciences of Belarus," Minsk (1991), pp. 69-76.
6. I. M. Zasyplin, I. A. Mishne, L. N. Baiduzha, and V. N. Fokin, in: *Low-Temperature Plasma Generators* [in Russian], Proc. of the XI All-Union Conf. on Low-Temperature Plasma Generators, Novosibirsk, Vol. 1 (1989), pp. 30-31.
7. A. F. Ainagos, G. M. Trunov, V. P. Lukashov, and B. A. Pozdnyakov, in: *Low-Temperature Plasma Generators* [in Russian], Proc. of the XI All-Union Conf. on Low-Temperature Plasma Generators, Vol. 1 (1989), pp. 59-60.
8. G. Yu. Dautov, Yu. S. Dudnikov, M. F. Zhukov, and G. M. Mustafin, *Zh. Prikl. Mekh. Tekh. Fiz.*, No. 1, 172-176 (1967).

9. A. S. An'shakov, G. Yu. Dautov, Yu. S. Dudnikov, et al., *Fiz. Khim. Obrab. Mater.*, No. 1, 27-32 (1969).
10. A. S. An'shakov, M. F. Zhukov, M. I. Sazonov, and A. N. Timoshevskii, *Izv. Sib. Otd. Akad. Nauk SSSR, Ser. Tekh. Nauk*, Issue 2, No. 8, 3-12 (1970).
11. Yu. V. Kurochkin and A. V. Pustogarov, in: *Experimental Studies of Plasma Generators [in Russian]*, Novosibirsk (1977), pp. 82-104.
12. A. S. Koroteev, A. M. Kostylev, V. V. Koba, et al., *Low-Temperature Plasma Generators [in Russian]*, Moscow (1969).
13. V. A. Lebsak, G. N. Machekhina, and G. N. Tikhomirov, *Installations with Electric-Arc Heating of Gas for Aerodynamic Investigations [in Russian]*, Survey of the Central Inst. of Aerohydrodynamics, No. 56, Moscow (1979), pp. 9-145.
14. ASD-TRD-62-729, Avco Corporation, Wilmington, MA (1963).
15. V. L. Sergeev, *Nonstationary Heat and Mass Transfer near the Stagnation Point [in Russian]*, Minsk (1988).
16. G. Yu. Dautov, *Zh. Prikl. Mekh. Tekh. Fiz.*, No.4, 106-110 (1963).
17. S. S. Kutateladze and O.I. Yas'ko, *Inzh.-Fiz. Zh.*, 7, No. 4, 25-28 (1964).
18. V. L. Sergeev, *Inzh.-Fiz. Zh.*, 9, No. 5, 657-666 (1965).
19. A. I. Zhidovich, O. A. Savel'ev, and O. I. Yas'ko, *Inzh.-Fiz. Zh.*, 11, No. 5, 625-630 (1966).
20. F. B. Yurevich, M. V. Volk-Levanovich, and A. G. Shashkov, *Inzh.-Fiz. Zh.*, 12, No. 6, 711-718 (1967).
21. G. Yu. Dautov, Yu. S. Dudnikov, and M. I. Sazonov, *Izv. Sib. Otd. Akad. Nauk SSSR, Ser. Tekh. Nauk*, Issue 3, No. 10, 56-63 (1965).
22. V. Ya. Smolyakov, *Zh. Prikl. Mekh. Tekh. Fiz.*, No. 1, 151-157 (1967).
23. V. L. Sergeev and V. E. Grushko, "A High-Enthalpy Plasma Generator for Tests of Heat-Shielding Materials in an Air Medium at Atmospheric Pressure," Preprint of the Academic Scientific Complex "Heat and Mass Transfer Institute of the Academy of Sciences of Belarus" (1993).
24. G. M. Bezladnov and V. L. Sergeev, *Izv. Akad. Nauk BSSR, Ser. Fiz.-Énerg. Nauk*, No. 3, 119-123 (1972).
25. M. F. Zhukov and Yu. I. Sukhinin, *Izv. Sib. Otd. Akad. Nauk SSSR, Ser. Tekh. Nauk*, Issue 1, No. 3, 55-61 (1969).
26. V. L. Sergeev and V. P. Terent'ev, *Izv. Akad. Nauk BSSR, Ser. Fiz.-Énerg. Nauk*, No. 2, 105-108 (1974).
27. V. L. Sergeev, A. S. Strogii, and V. A. Tsurko, *Inzh.-Fiz. Zh.*, 42, No. 1, 34-39 (1982).